Vietnam Journal of Science and Technology ***64***(2) (2026) 375–394
DOI: https://doi.org/10.15625/2525-2518/21672

An analytical solution to neutral axis-based free vibration of temperature-dependent functionally graded beam

Nguyen Ngoc Huyen[1,*], Do Nam[2], Vadim Kudryashov[3], Nguyen Tien Khiem[4,*]

[1]*Thuy Loi University, 175, Tay Son, Kim Lien ward, Ha Noi, Viet Nam*
[2]*VNU University of Engineering and Technology, 144 Xuan Thuy, Cau Giay ward, Hanoi, Viet Nam*
[3]*University of Civil Protection, Ministry for Emergency Situations, 25 Mashinostroiteley Str., Mínsk 220118, Belarus*
[4]*Institute of Mechanics, VAST, 264 Doi Can, Ngoc Ha ward, Ha Noi, Viet Nam*

[*]Email: *nnhuyen@tlu.edu.vn; ntkhiem@imech.vast.vn*

Received: 06 October 2024; Accepted for publication: 24 October 2024

Abstract. The present study is devoted to analysis of neutral axis effect on fundamental frequency of functionally graded Euler-Bernoulli beams with temperature-dependent properties under nonlinear temperature rise distribution. First, a formula for exact position of the neutral axis in the beams is derived for general nonlinear temperature distribution and power law of material gradation. Then, the dislocation of the neutral axis from the central one is examined along volume fraction index and various types of the temperature distribution. Finally, the effect of exact neutral axis position on fundamental frequency is investigated to reveal when the neutral axis position and nonlinear temperature distribution should be considered in vibration analysis of the beams. Numerical analysis is conducted for illustration of the proposed theoretical development.

Keywords: functionally graded material, Euler-Bernoulli beam, neutral axis, thermal effect, free vibration.

Classification numbers: 5.4.2, 5.4.3, 5.4.5.

1. INTRODUCTION

Functionally Graded Materials (FGM) are usually made of ceramics and metals to enhance the thermal protection and load-carrying capability of structures such as space vehicles, aircraft, nuclear power plants, etc. The fundamentals of modeling and analysis of FGMs and FGM structures were provided in [1].

A lot of studies on the dynamics of functionally graded (FG) beams were completed without thermal effects using different approaches such as analytical [2-4], Rayleigh-Ritz [5, 6], finite element [7, 8] and spectral element [9, 10] methods. While most authors of the previous studies have established models of FG beams using the mid-plane instead of the neutral surface, Yaghoobi and Fereidoon [11] obtained an attractive formula for the exact position of neutral surface in FG beams with the power law of material gradation. They have shown that dislocation of the neutral axis (NA) from the central one decreases when the ratio between

ceramic and metal modulus is decreasing, and the volume fraction index is increasing. The authors demonstrated also that static deflection based on the neutral axis gets to be larger than that obtained with the central axis (CA). Later, Eltaher *et al*. [12] and Chen and Chang [13] established again the formula for the exact position of NA and thoroughly studied its influence on natural frequencies of FG beams with various modulus ratios, volume fraction index, and for different boundary conditions. They reconfirmed that considering the neutral axis leads to beam stiffness reduction and the deviation of natural frequencies calculated for NA and CA can be more than 10 % in certain case. While the results mentioned above were obtained for functionally graded Euler-Bernoulli beams, a comprehensive modal analysis of functionally graded beams based on the neutral axis conception were accomplished for Timoshenko beams in [14]. Then, a general approach to free and forced vibrations of cracked functionally graded Timoshenko beams was developed in [15].

As mentioned above, with thermal protection purposes, the behavior of FGM structures with temperature-dependent properties and under thermal load must be thoroughly studied. The primary important problems in thermo-mechanical analysis of FGM structures such as beams, plates, and shells were formulated in [16-20]. Alshorbagy [21] using the third order shear deformation beam theory and Finite Element Method (FEM) studied the temperature effect on natural frequencies and mode shapes of FG beams and has shown that dimensionless natural frequencies decrease with an increase in both material gradation index and temperature. He has showed also that the temperature effect on high frequencies is greater than on the lower ones and mode shapes are almost unaffected by the temperature. However, there was considered in this study only uniform temperature distribution along the beam thickness. Chen *et al.* [22] investigated variations of the fundamental frequency of FGM beams with general boundary conditions based on the different high-order shear deformation beam theories and various temperature distributions including the uniform, linear, and nonlinear distributions across beam thickness. The latter authors proved that the fundamental frequency of heated FGM beams decreases with temperature rise according to either linear (LTD) or nonlinear (NLTD) temperature distributions and discrepancy between natural frequencies computed by LTD and NLTD become more noticeable when difference between temperatures at the top and bottom beam surfaces increases. Mahi *et al.* [23] formulated the thermo-mechanical free vibration problem of symmetric FG beams based on different high-order shear deformation beam theories and various laws of material gradation such as power, exponential and sigmoid ones. The natural frequencies computed by using the beam theories and material gradation laws are compared along slenderness ratio (L/h), volume fraction index and temperature imposed at top and bottom surfaces of the symmetric beam. Ebrahimi *et al*. [24] studied the fundamental frequency of FGM Euler-Bernoulli beam with porosity under thermal loads and demonstrated that porosity in the FGM increases the beam frequency regardless of temperature distributions, while an increase in both temperature and material gradation index leads to the frequency reduction. Malekzadeh and his co-workers examined dynamic response of functionally graded beams subjected to thermal and moving load [25] and moving heat source [26]. In the former study, the authors stated that the material temperature-dependent properties significantly affect the dynamic response of FG beams and cannot be ignored in the dynamic analysis. In the latter work, the two-dimensional heat conduction equation was solved to obtain a nonstationary temperature distribution, and its solution was employed to study the dynamic response of a Timoshenko FG beam under a moving heat source. It was found that material gradation index greatly affects the temperature distribution and temperature-dependent properties of material have a significant effect on the beam response. Both the free vibration and thermal buckling of FGM beams were studied in [27-30], where critical buckling temperature was determined for

FG beams under various types of thermal loading [27]; the heated temperature-dependent FGM beams [28, 29] and high-order strain deformable FG beams under both thermal and mechanical loads [30]. The buckling and post-buckling of porous Timoshenko FGM beams under uniform temperature distribution were examined in [31]. Thermomechanical vibration of Euler-Bernoulli functionally graded nanobeams was investigated in [32] where the effect of various factors such as non-local parameters, gradient index, temperature-dependent material properties, thermal effects on the beam's fundamental frequency was thoroughly studied. Buckling of functionally graded beams bonded with piezoelectric layers under thermal load and voltage was considered in [33] where the authors revealed that the critical buckling temperature of the piezoelectric beam under linear temperature rise is greater than that of the beam under nonlinear one. Natural frequencies of temperature-dependent FGM plates under various types of thermal loads were examined in [34-37], where a common conclusion was exposed that natural frequencies of the ceramic/metal plates decrease with material gradation index. It is interesting to note the study accomplished in [37] where the problem of thermal buckling of FGM plate has been formulated by considering the physical neutral surface instead of mid-plane as was done in most of the earlier published works. However, the formula derived for the physical position of the neutral surface is valid only for the uniform temperature distribution. The same situation can be found in [38] where the shear correction factor for temperature-dependent functionally graded beams was investigated also based on the neutral surface concept. To the authors' knowledge, the exact position of neutral axis in functionally graded beams under thermal load varying across beam thickness and its effect on vibration of the temperature-dependent FGM beam structures have not been published in the literature.

Thus, in the present study, the free vibration problem is formulated for temperature-dependent FGM Euler-Bernoulli beams based on the neutral surface concept and the power law of material gradation. First, a formula for calculating the exact position of neutral axis in FGM beams with temperature-dependent properties varying according to the power law is derived for general nonlinear temperature distribution across beam thickness. Then, dislocation of the neutral axis from the central one is examined along material grading index and various types (uniform, linear and nonlinear) temperature distribution field. Finally, the effect of the neutral axis position on fundamental frequency is numerically investigated for simply supported FGM beam.

2. MODEL OF FGM BEAMS WITH TEMPERATURE-DEPENDENT PROPERTIES

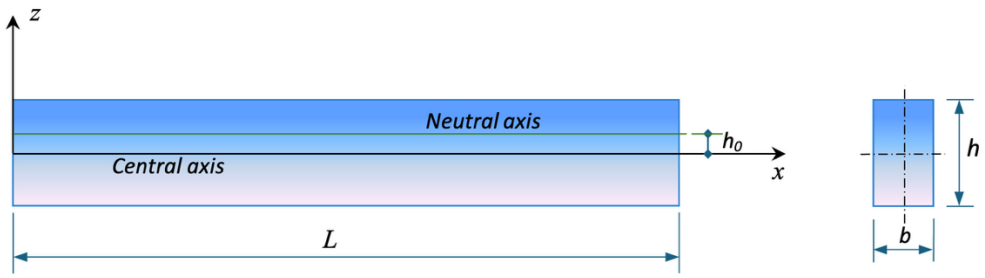

Figure 1. Model of functionally graded beam.

Consider a beam of length L, cross-section area $A = b \times h$, as shown in Figure 1, that is made of FGM with material properties varying along thickness by the power law:

$$P(z,T) = P_b(T) + [P_t(T) - P_b(T)]\left(z/h + 1/2\right)^p, -h/2 \le z \le h/2 \tag{1}$$

where P stands for E, G and ρ, the elasticity, shear modulus and material density at the top (with index t) and bottom (with index b) respectively; z is ordinate from the central axis, T is the temperature field. Dependence of material properties on temperature is defined by

$$P(T) = P_0\left[P_{-1}/T + 1 + P_1 T + P_2 T^2 + P_3 T^3\right] \tag{2}$$

with coefficients $P_0, P_{-1}, P_1, P_2, P_3$ are given specifically for material constituents (Table 1).

Table 1. Temperature dependent materials constants [25].

Material	Properties	P_0	P_{-1}	P_1	P_2	P_3
Al_2O_3	E (Pa)	349.55e+9	0	-3.853e-4	4.027e-7	-1.673e-10
	ρ (kg/m^3)	3800	0	0	0	0
	α (1/K)	6.8269e-6	0	1.838e-4	0	0
	κ (Wm/K)	-14.087	0	0	0	0
SUS304	E (Pa)	201.04e+9	0	3.079e-4	-6.534e-7	0
	ρ (kg/m^3)	8166	0	0	0	0
	α (1/K)	12.330e-6	0	8.085e-4	0	0
	κ (Wm/K)	15.379	0	0	0	0

According to Euler-Bernoulli beam theory, the displacement fields in the cross-section at x are

$$u(x,z,t) = u_0(x,t) - (z - h_0)\partial w(x,t)/\partial x; w(x,z,t) = w_0(x,t) \tag{3}$$

with $u_0(x,t), w_0(x,t)$ being the displacements of neutral axis that is located at the height h_0 from the central axis. Therefore, constitutive equations get the form

$$\varepsilon_x = \partial u_0/\partial x - (z - h_0)\partial^2 w/\partial x^2 \tag{4}$$

and

$$\sigma_x = E(z,T)\varepsilon_x \tag{5}$$

The stress due to temperature rise is

$$\sigma_x^T = -E(z,T)\alpha(z,T)\nabla T(z), \tag{6}$$

where $\alpha(z,T)$ is thermal expansion coefficient and $\nabla T(z)$ is the change in temperature versus the beam thickness that will be determined later.

Using the constitutive equations (3)–(6), strain and kinetic energies are defined as

$$U_S = \frac{1}{2}\int_V \left(\sigma_x \varepsilon_x\right) dV; U_T = \frac{1}{2}\int_V \sigma_x^T w_x^2 dV; \quad K = \frac{1}{2}\int_V \rho\left(z,T\right)\left(u_t^2 + w_t^2\right) dV \tag{7}$$

and finally, one obtains

$$U=\frac{1}{2}\int_0^L\int_A \sigma_x\varepsilon_x dAdx=\frac{1}{2}\int_0^L\Big[A_{11}u_{0,x}^2-2A_{12}u_{0,x}w_{0,xx}+A_{22}w_{0,xx}^2-A_T w_{0,x}^2\Big]dx$$

$$K=\frac{1}{2}\int_0^L\int_A \rho\left(u_t^2+w_t^2\right)dAdx=\frac{1}{2}\int_0^L\Big[I_{11}\left(u_{0,t}^2+w_{0,t}^2\right)+2I_{12}u_{0,t}w_{0,xt}+I_{22}w_{0,xt}^2\Big]dx \tag{8}$$

where

$$\{A_{11},A_{12},A_{22}\}=\int_A E(z,T)\left\{1,z-h_0,(z-h_0)^2\right\}dA;$$

$$A_T=\int_A E(z,T)\alpha(z,T)\Delta T(z)dA;\ \{I_{11},I_{12},I_{22}\}=\int_A \rho(z)\left\{1,z-h_0,(z-h_0)^2\right\}dA \tag{9}$$

Now, using the Hamilton principle allows one to derive equations of motion for the beam in the form

$$\begin{aligned}&I_{11}\ddot{u}_0-I_{12}\ddot{w}_{0,x}-A_{11}u_{0,x}+A_{12}w_{0,xxx}=0;\\&I_{11}\ddot{w}_0+I_{12}\ddot{u}_{0,x}-I_{22}\ddot{w}_{0,xx}-A_{12}u_{0,xxx}+A_{22}w_{0,xxx}-A_T w_{0,xx}=0\end{aligned} \tag{10}$$

By introducing the displacement amplitudes

$$\left\{U\left(x,\omega\right),W\left(x,\omega\right)\right\}=\int_{-\infty}^{\infty}\{u_0(x,t),w_0(x,t)\}e^{-i\omega t}dt \tag{11}$$

Eqs. (10) are transformed to the frequency domain as

$$\begin{aligned}&(A_{11}U_{xx}+\omega^2 I_{11}U)-(A_{12}W_{xxx}+\omega^2 I_{12}W_x)=0;\\&A_{22}W_{xxxx}+(\omega^2 I_{22}-A_T)W_{xx})-\omega^2 I_{11}W-(A_{12}U_{xxx}+\omega^2 I_{12}U_x)=0\end{aligned} \tag{12}$$

3. MODEL OF TEMPERATURE RISE DISTRIBUTION

Suppose that thermal conductivity of the FGM is independent upon temperature and varies along beam thickness according also to the power law as [23]

$$k(z)=k_b+(k_t-k_b)(z/h+1/2)^p, \tag{13}$$

where k_t,k_b are thermal conductivity of the top and bottom materials, respectively. Therefore, solution of one-dimensional equation for steady-state heat conduction given by [22, 23]

$$\frac{d}{dz}\left(k(z)\frac{dT}{dz}\right)=0 \tag{14}$$

can be found in the form

$$T(z)=T_b+(T_t-T_b)\nabla T(z)=T_b+T_{t-b}\nabla T(z);T_{t-b}=T_t-T_b=\Delta T, \tag{15}$$

where

$$\nabla T\left(z\right)=T_b+T_{t-b}\left[\int_{-h/2}^{z}dz/k\left(z\right)/\int_{-h/2}^{h/2}dz/k\left(z\right)\right].$$

Using expression (13) the integral

$$\zeta(z)=\int_{-h/2}^{z} dz/k(z)=\int_{-h/2}^{z}\frac{dz}{k_b+(k_t-k_b)(z/h+1/2)^p}$$

can be calculated as

$$\zeta(z)=\sum_{n=0}^{\infty}\left\{\frac{(-1)^n}{np+1}\left[\frac{k_t-k_b}{k_b}\right]^n\left(\frac{z}{h}+\frac{1}{2}\right)^{np+1}\right\}$$

Therefore, one gets

$$C=\int_{-h/2}^{h/2} dz/k(z)=\zeta(h/2)=\sum_{n=0}^{\infty}\left\{\frac{(-1)^n}{np+1}\left[\frac{k_t-k_b}{k_b}\right]^n\right\} \tag{16}$$

and finally, we obtain

$$\nabla T(z)=\frac{(z/h+1/2)}{C}\sum_{n=0}^{\infty}\left\{\frac{(-1)^n}{np+1}\left[\frac{k_t-k_b}{k_b}\right]^n\left(\frac{z}{h}+\frac{1}{2}\right)^{np}\right\} \tag{17}$$

Taking only the first term with $n=0$ in the series (17) leads to the case of linear temperature rise as

$$\nabla T(z)=V_1(z)=(z/h+1/2). \tag{18}$$

In some studies, the series (16) is truncated by a finite number N of terms,

$$\nabla T(z)=\frac{(z/h+1/2)}{C}\sum_{n=0}^{N}\left\{\frac{(-1)^n}{np+1}\left[\frac{k_t-k_b}{k_b}\right]^n\left(\frac{z}{h}+\frac{1}{2}\right)^{np}\right\} \tag{19}$$

and $N=5$ was taken in many studies, for example [30, 33], etc.

4. EXACT POSITION OF NEUTRAL AXIS IN TEMPERATURE-DEPENDENT FGM BEAMS

As well-known, exact position of neutral surface is determined from condition

$$\int_{-h/2}^{h/2} E(z,T)[z-h_0]dz=0 \tag{20}$$

that gives rise to

$$h_0=\int_{-h/2}^{h/2} E(z,T)zdz\Big/\int_{-h/2}^{h/2} E(z,T)dz \tag{21}$$

To calculate the exact position of neutral surface defined by Eq. (21), we need first to express the constant $E(z,T)$ as function of z as following

$$E(z,T)=E_b(T)+[E_t(T)-E_b(T)](z/h+1/2)^p \tag{22}$$

where

$$E_b(T)=E_0^b\left(1+E_1^bT+E_2^bT^2+E_3^bT^3\right);\ E_t(T)=E_0^t\left(1+E_1^tT+E_2^tT^2+E_3^tT^3\right) \tag{23}$$

with coefficients $E_k^t, E_k^b, k = 0, 1, 2, 3$ are given in Table 1 for chosen top and bottom materials. Using the latter expressions, one can calculate

$$E_t(T) - E_b(T) = E_0^{t-b}\left(1 + E_1^{t-b}T + E_2^{t-b}T^2 + E_3^{t-b}T^3\right) \tag{24}$$

where the following notations are used

$$E_0^{t-b} = E_0^t - E_0^b; \quad E_k^{t-b} = \left(E_0^t E_k^t - E_0^b E_k^b\right) / E_0^{t-b}, k = 1, 2, 3$$

Putting (15) into (23) and (24), one obtains

$$\begin{aligned} E_b(T) &= E_0^b\left(Q_0^b + Q_1^b \nabla T + Q_2^b \nabla T^2 + Q_3^b \nabla T^3\right) \\ E_t(T) - E_b(T) &= E_0^{t-b}\left(Q_0^{t-b} + Q_1^{t-b} \nabla T + Q_2^{t-b} \nabla T^2 + Q_3^{t-b} \nabla T^3\right) \end{aligned} \tag{25}$$

where the following notations are introduced

$$\bar{E}_k^b = E_0^b Q_k^b; \bar{E}_k^t = E_0^t Q_k^t; \bar{E}_k^{t-b} = E_0^{t-b} Q_k^{t-b} = \bar{E}_k^t - \bar{E}_k^b, k = 0,1,2,3 \tag{26}$$

$$Q_0^b = 1 + E_1^b T_b + E_2^b T_b^2 + E_3^b T_b^3, Q_0^{t-b} = 1 + E_1^{t-b} T_b + E_2^{t-b} T_b^2 + E_3^{t-b} T_b^3$$

$$\begin{aligned} \begin{Bmatrix} Q_1^{t,b} \\ Q_1^{t-b} \end{Bmatrix} &= T_{t-b}\left[\begin{Bmatrix} E_1^{t,b} \\ E_1^{t-b} \end{Bmatrix} + 2T_b \begin{Bmatrix} E_2^{t,b} \\ E_2^{t-b} \end{Bmatrix} + 3T_b^2 \begin{Bmatrix} E_3^{t,b} \\ E_3^{t-b} \end{Bmatrix}\right] \\ \begin{Bmatrix} Q_2^b \\ Q_2^{t-b} \end{Bmatrix} &= T_{t-b}^2\left[\begin{Bmatrix} E_2^b \\ E_2^{t-b} \end{Bmatrix} + 3T_b \begin{Bmatrix} E_3^b \\ E_3^{t-b} \end{Bmatrix}\right]; \begin{Bmatrix} Q_3^b \\ Q_3^{t-b} \end{Bmatrix} = T_{t-b}^3 \begin{Bmatrix} E_3^b \\ E_3^{t-b} \end{Bmatrix} \end{aligned} \tag{27}$$

Substituting (25) into (22) yields

$$\begin{aligned} E(z,T) = &\left[\bar{E}_0^b + \bar{E}_0^{t-b} V_p(z)\right] + \left[\bar{E}_1^b + \bar{E}_1^{t-b} V_p(z)\right] \nabla T(z) + \\ &+ \left[\bar{E}_2^b + \bar{E}_2^{t-b} V_p(z)\right] \nabla T^2(z) + \left[\bar{E}_3^b + \bar{E}_3^{t-b} V_p(z)\right] \nabla T^3(z), \end{aligned} \tag{28}$$

Particularly, in case of uniform temperature distribution: $\Delta T = T_t - T_b = T_{t-b} = 0$ or $T_b = T_t = T_0$ one has

$$Q_1^b = Q_2^b = Q_3^b = Q_1^{t-b} = Q_2^{t-b} = Q_3^{t-b} = 0 \tag{29}$$

Therefore, one obtains the constants for uniform temperature distribution as

$$E_u(z,T) = \left[E_0^b Q_0^b + E_0^{t-b} Q_0^{t-b} V_p(z)\right] \tag{30}$$

and exact position of neutral surface measured from the mid-plane can be calculated as [34, 35]

$$h_0 = \int_{-h/2}^{h/2} E(z,T)\, z\, dz \Big/ \int_{-h/2}^{h/2} E(z,T)\, dz = \frac{ph\left(\bar{E}_0^t - \bar{E}_0^b\right)}{2(p+2)\left(\bar{E}_0^t + p\bar{E}_0^b\right)} \tag{31}$$

where

$$\bar{E}_0^b = E_0^b Q_0^b = E_0^b\left(1 + E_1^b T_0 + E_2^b T_0^2 + E_3^b T_0^3\right); \bar{E}_0^t = E_0^t Q_0^t = E_0^t\left(1 + E_1^t T_0 + E_2^t T_0^2 + E_3^t T_0^3\right) \tag{32}$$

Obviously, for homogeneous beams with $p = 0$ or $E_0^t = E_0^b$, Eq. (31) yields $h_0 = 0$ that implies overlap of the neutral surface with the central one. Furthermore, ignoring the thermal effect in expressions (32), Eq. (31) leads to the formulae obtained earlier in [12-14].

In general case, denoting

$$\nabla T(z)=\sum_{n=0}^{\infty}\delta_n V^{np+1};\ \delta_n=\frac{(-1)^n}{(np+1)C}\left[\frac{k_t-k_b}{k_b}\right]^n;\ V(z)=(z/h+1/2)$$

the expression (28) can be rewritten as

$$E(z,T)=\left[\bar{E}_0^b+\bar{E}_0^{t-b}V^p(z)\right]+\sum_{n=0}^{\infty}\delta_n\left[\bar{E}_1^b+\bar{E}_1^{t-b}V^p(z)\right]V^{np+1}+\sum_{n_1,n_2=0}^{\infty}\delta_{n_1}\delta_{n_2}\left[\bar{E}_2^b+\bar{E}_2^{t-b}V^p(z)\right]V^{(n_1+n_2)p+2}$$

$$+\sum_{n_1,n_2,n_3=0}^{\infty}\delta_{n_1}\delta_{n_2}\delta_{n_3}\left[\bar{E}_3^b+\bar{E}_3^{t-b}V^p(z)\right]V^{(n_1+n_2+n_3)p+3}$$

or

$$E(z,T)=\sum_{k=0}^{3}\sum_{n_1,\ldots,n_k=0}^{\infty}\delta_{n_1}\ldots\delta_{n_k}\left[\bar{E}_k^bV^{m_k}(z)+\bar{E}_k^{t-b}V^{m_k+p}(z)\right] \tag{33}$$

with $m_0=0;\ m_1=np+1;m_2=(n_1+n_2)p+2;m_3=(n_1+n_2+n_3)p+3$. So, one can calculate the integrals

$$\int_{-h/2}^{h/2}E(z,T)dz=h\psi_0\left(p,\bar{E}_0^t,\bar{E}_0^b,\ldots,\bar{E}_3^t,\bar{E}_3^b\right);\ \int_{-h/2}^{h/2}E(z,T)zdz=h^2\psi_1\left(p,\bar{E}_0^t,\ldots,\bar{E}_3^t,\bar{E}_0^b,\ldots,\bar{E}_3^b\right) \tag{34}$$

where functions $\psi_0\left(p,\bar{E}_k^t,\bar{E}_k^b\right)$ and $\psi_1\left(p,\bar{E}_k^t,\bar{E}_k^b\right)$ are given in Appendix I. Therefore, the exact position of neutral axis in general case can be calculated as

$$h_0=\int_{-h/2}^{h/2}E(z,T)\,z\,dz\ /\ \int_{-h/2}^{h/2}E(z,T)\,dz=\frac{h\psi_1\left(p,\bar{E}_0^b,\bar{E}_1^b,\bar{E}_2^b,\bar{E}_3^b,\bar{E}_0^t,\bar{E}_1^t,\bar{E}_2^t,\bar{E}_3^t\right)}{\psi_0\left(p,\bar{E}_0^b,\bar{E}_1^b,\bar{E}_2^b,\bar{E}_3^b,\bar{E}_0^t,\bar{E}_1^t,\bar{E}_2^t,\bar{E}_3^t\right)} \tag{35}$$

To check for validity of the later formula, first, we consider the case when material properties are independent upon temperature, $\bar{E}_k^b=\bar{E}_k^t=0,k=1,2,3$. Then,

$$\psi_0\left(p,\bar{E}_k^t,\bar{E}_k^b\right)=\frac{\bar{E}_0^t+p\bar{E}_0^b}{p+1};\ \psi_1\left(p,\bar{E}_k^t,\bar{E}_k^b\right)=\frac{p\left(\bar{E}_0^t-\bar{E}_0^b\right)}{2(p+1)(p+2)}$$

that lead the formulae (35) to (31). Furthermore, in case of linear distribution of temperature, when $T(z)=T_b+(T_t-T_b)V(z)$, one will have got

$$\psi_0\left(p,\bar{E}_k^t,\bar{E}_k^b\right)=\sum_{m=0}^{3}\frac{(m+1)\bar{E}_m^t+p\bar{E}_m^b}{(m+1)(m+1+p)}$$

$$\psi_1\left(p,\bar{E}_k^t,\bar{E}_k^b\right)=\sum_{m=0}^{3}\frac{(m+1)(m+2)(m+p)\bar{E}_m^t-p\left(2-m^2-mp\right)\bar{E}_m^b}{2(m+1)(m+2)(m+p+1)(m+p+2)} \tag{36}$$

So that

$$h_0=h\sum_{m=0}^{3}\frac{(m+1)(m+2)(m+p)\bar{E}_m^t-p\left(2-m^2-mp\right)\bar{E}_m^b}{2(m+1)(m+2)(m+p+1)(m+p+2)}\ /\ \sum_{m=0}^{3}\frac{(m+1)\bar{E}_m^t+p\bar{E}_m^b}{(m+1)(m+1+p)} \tag{37}$$

5. FREE VIBRATION OF TEMPERATURE-DEPENDENT FGM BEAMS

It is obvious that the exact position of neutral axis has been determined from condition (20) which implies vanishing constant $A_{12}=0$. So, Eqs. (12) are reduced to

$$\begin{aligned} A_{11}U_{xx}+\omega^2 I_{11}U-\omega^2 I_{12}W_x&=0\\ A_{22}W_{xxxx}+(\omega^2 I_{22}-A_T)W_{xx}-\omega^2 I_{11}W-\omega^2 I_{12}U_x&=0 \end{aligned} \tag{38}$$

Seeking solution of Eq. (38) in the form $\{U(x,\omega),W(x,\omega)\}^T=\{U_0(\omega),W_0(\omega)\}^T e^{\lambda x}$ allows one to obtain the equation

$$\left[\mathbf{A}(\lambda)\right]\{U_0(\omega),W_0(\omega)\}^T=\{0\} \tag{39}$$

with

$$\left[\mathbf{A}(\lambda)\right]=\begin{bmatrix} \lambda^2 A_{11}+\omega^2 I_{11} & -\omega^2 I_{12}\lambda \\ -\omega^2 I_{12}\lambda & \lambda^4 A_{22}+\lambda^2\left(\omega^2 I_{22}-A_T\right)-\omega^2 I_{11} \end{bmatrix}.$$

The condition for existence of nontrivial solution of Eq. (39) leads to the so-called characteristic equation

$$\det\left[\mathbf{A}(\lambda)\right]=a\lambda^6+b\lambda^4+c\lambda^2+d=0 \tag{40}$$

where

$$a=A_{11}A_{22};\ b=A_{11}\left(\omega^2 I_{22}-A_T\right)+\omega^2 I_{11}A_{22};\ c=\omega^2 I_{11}\left(\omega^2 I_{22}-A_{11}-A_T\right)-\omega^4 I_{12}^2; d=-\omega^4 I_{11}^2$$

It can be seen from the characteristic equation (40) that its six roots can be found from three roots η_1,η_2,η_3 of the cubic equation $a\eta^3+b\eta^2+c\eta+d=0$, as

$$\lambda_{1,4}=\pm k_1;\lambda_{2,5}=\pm k_2;\ \lambda_{3,6}=\pm k_3, k_r=\sqrt{\eta_r}, r=1,\,2,\,3.$$

Hence, general solution of Eq. (38) can be expressed as

$$\begin{Bmatrix} U(x) \\ W(x) \end{Bmatrix}=\begin{bmatrix} \beta_1 e^{k_1 x} & \beta_2 e^{k_2 x} & \beta_3 e^{k_3 x} & -\beta_1 e^{-k_1 x} & -\beta_2 e^{-k_2 x} & -\beta_3 e^{-k_3 x} \\ e^{k_1 x} & e^{k_2 x} & e^{k_3 x} & e^{-k_1 x} & e^{-k_2 x} & e^{-k_3 x} \end{bmatrix}\{C\}, \tag{41}$$

where $\{C\}=\{C_1,...,C_6\}^T$ is vector of constants and $\beta_r=\left[\lambda_r\omega^2 I_{12}/\left(\omega^2 I_{11}+\lambda_r^2 A_{11}\right)\right]; r=1,\,2,\,3.$

Applying given boundary conditions for solution (40) allows one to determine constants $C_1,...,C_6$ and therefore natural frequencies and mode shapes. Namely, for simply supported beam the boundary conditions are $U(0)=W(0)=W''(0)=U'(L)=W(L)=W''(L)=0$ that leads to equations

$$\left[\mathbf{B}_{SS}(\omega)\right]\{C\}=\{0\}, \tag{42}$$

where matrix

$$\left[\mathbf{B}_{SS}(\omega)\right]=\begin{bmatrix} \beta_1 & \beta_2 & \beta_3 & -\beta_1 & -\beta_2 & -\beta_3 \\ 1 & 1 & 1 & 1 & 1 & 1 \\ k_1^2 & k_2^2 & k_3^2 & k_1^2 & k_2^2 & k_3^2 \\ k_1\beta_1 e^{k_1 L} & k_2\beta_2 e^{k_2 L} & k_3\beta_3 e^{k_3 L} & k_1\alpha_1 e^{-k_1 L} & k_2\beta_2 e^{-k_2 L} & k_3\beta_3 e^{-k_3 L} \\ e^{k_1 L} & e^{k_2 L} & e^{k_3 L} & e^{-k_1 L} & e^{-k_2 L} & e^{-k_3 L} \\ k_1^2 e^{k_1 L} & k_2^2 e^{k_2 L} & k_3^2 e^{k_3 L} & k_1^2 e^{-k_1 L} & k_2^2 e^{-k_2 L} & k_3^2 e^{-k_3 L} \end{bmatrix} \tag{43}$$

For existence of nontrivial constant vector $\{C\}$ it must be satisfied condition

$$\det\left[\mathbf{B}(\omega)\right]=0, \tag{44}$$

that is so-called frequency equation for finding natural frequencies $\omega_1,\omega_2,\omega_3,...$ of the FGM beam. It should be noted here that among the natural frequencies, there are found natural frequencies of both axial and flexural vibration modes which are distinguished only by vibration mode shapes. In case of clamped beams with boundary conditions

$$U(0)=W(0)=W'(0)=U(L)=W(L)=W'(L)=0$$

the matrix $\mathbf{B}(\omega)$ in Eq. (42) has the form

$$\left[\mathbf{B}_{CC}(\omega)\right]=\begin{bmatrix} \beta_1 & \beta_2 & \beta_3 & -\beta_1 & -\beta_2 & -\beta_3 \\ 1 & 1 & 1 & 1 & 1 & 1 \\ k_1 & k_2 & k_3 & -k_1 & -k_2 & -k_3 \\ \beta_1 e^{k_1 L} & \beta_2 e^{k_2 L} & \beta_3 e^{k_3 L} & -\beta_1 e^{-k_1 L} & -\beta_2 e^{-k_2 L} & -\beta_3 e^{-k_3 L} \\ e^{k_1 L} & e^{k_2 L} & e^{k_3 L} & e^{-k_1 L} & e^{-k_2 L} & e^{-k_3 L} \\ k_1 e^{k_1 L} & k_2 e^{k_2 L} & k_3 e^{k_3 L} & -k_1 e^{-k_1 L} & -k_2 e^{-k_2 L} & -k_3 e^{-k_3 L} \end{bmatrix} \tag{45}$$

After natural frequencies $\omega_1,\omega_2,\omega_3,...$ of the beams and normalized solution $\{\zeta^k\}=\{\zeta_1^k,...,\zeta_6^k\}^T$ of equation

$$\left[\mathbf{B}(\omega_k)\right]\{\zeta^k\}=\{0\} \tag{46}$$

have been found, mode shape corresponding to natural frequency ω_k can be calculated as

$$\begin{Bmatrix} U_k(x) \\ W_k(x) \end{Bmatrix}=\theta_k\begin{bmatrix} \beta_1 e^{k_1 x} & \beta_2 e^{k_2 x} & \beta_3 e^{k_3 x} & -\beta_1 e^{-k_1 x} & -\beta_2 e^{-k_2 x} & -\beta_3 e^{-k_3 x} \\ e^{k_1 x} & e^{k_2 x} & e^{k_3 x} & e^{-k_1 x} & e^{-k_2 x} & e^{-k_3 x} \end{bmatrix}\{\zeta^k\} \tag{47}$$

The arbitrary constant θ_k can be determined from normalization condition

$$\max_{x\in[0,L]}\{W_k(x)\}=1 \tag{48}$$

6. NUMERICAL RESULTS AND DISCUSSION

6.1. Theory validation

First, for validation of the above proposed theory, non-dimensional fundamental frequency, $\bar{\omega} = \omega(L^2 / h)\sqrt{\rho_b / E_b}$, is computed for temperature-independent FGM beam made of Al_2O_3 in top and stainless steel SUB304 at bottom. In this particular example, the frequency is computed in two cases: with the exact position of neutral axis and with the central axis denoted respectively by NA and CA for simply supported (SS) beam. Both the results are compared to those obtained by Simsek [5] where the central axis is considered instead of the neutral one. The results presented in Table 2 show that the CA-frequency computed in the present study is agreed with those given in [5]. Also, the comparison between NA-frequency and CA-frequency demonstrates a noticeable effect of the exact position of neutral axis on computed fundamental frequency even in the case of temperature-independent FGM beams. Namely, in the above particular case, calculated CA-frequency is greater than NA-frequency for every material grading index.

Table 2. Comparison of dimensionless fundamental frequency computed for simply supported (SS) FGM beams without thermal effects.

L/h	*p* (V.F.I)	0.1	0.2	0.5	1.0	2.0	5.0	10.0
5	Simsek [5]	n.a.	5.0219	4.5936	4.1483	3.7793	3.5948	3.4920
	Present CA	5.3087	5.0235	4.5072	4.1106	3.7971	3.5095	3.3535
	Present NA	5.2976	4.9890	4.3956	3.9260	3.6009	3.4022	3.3081
20	Simsek [5]	n.a.	5.0980	4.6645	4.2163	3.8471	3.6628	3.5546
	Present CA	5.3676	5.0829	4.5676	4.1717	3.8587	3.5715	3.5715
	Present NA	5.3566	5.0489	4.5676	3.9901	3.6658	3.4662	3.3718

Notice: V.F.I – Volume fraction index; CA – Central axis; NA – Neutral axis.

Table 3. Comparison of dimensionless fundamental frequency computed for simply supported (SS) FGM beams with thermal effects.

ΔT	*p* (V.F.I)	0.1		0.2		0.5	
	Temp. Dist.	*LTR*	*NTR*	*LTR*	*NTR*	*LTR*	*NTR*
20K	Ref. [24]	4.7055	4.7018	4.4413	4.4333	3.9553	3.9353
	Present CA	4.7124	4.7242	4.4612	4.4780	4.0072	4.0297
	Present NA	4.7067	4.7187	4.4408	4.4578	3.9367	3.9593
40K	Ref. [24]	4.6110	4.6020	4.3452	4.3278	3.8553	3.8140
	Present CA	4.5981	4.6220	4.3490	4.3839	3.8974	3.9477
	Present NA	4.5935	4.6177	4.3305	4.3661	3.8298	3.8811
80K	Ref. [24]	4.1476	4.3956	4.1476	4.1087	3.6458	3.5590
	Present CA	4.4047	4.4551	4.1509	4.2292	3.6819	3.8090
	Present NA	4.4015	4.4523	4.1352	4.2148	3.6188	3.7484

Notice: LTR, NTR – Linear and nonlinear temperature rise distribution.

In case of temperature-dependent Euler-Bernoulli FGM beam, fundamental frequencies computed for various volume fraction index $p = 0.1, 0.2, 0.5$ and linear and nonlinear

temperature rise with $\Delta T = 20, 40, 80$ Kare compared to that obtained by Ebrahimi *et al*. [24]. Since the results given in [24] are CA-frequencies, there are not only the CA-frequencies provided in Table 3 but also NA-frequencies that are both computed in this study for temperature dependent FGM beam with simple end supports. Noticeably, the CA-frequencies are almost close to the compared ones, but there are observed some deviation, for example, in case of high temperature rise (ΔT = 80 K). The deviations can be explained by the fact that in the present study the thermal conductivity is assumed to be temperature independent for both ceramic and metal as shown in Table 1. The results provided in the table show also that the fundamental frequency computed with central axis-based theory is overestimated in comparison with that obtained by using exact position of neutral axis.

6.2. Exact position of neutral axis

The exact position of the neutral axis denoted by NA-position is calculated as a function of the volume fraction index and temperature for simply supported Al_2O_3/SUB304 beam and results are presented in Figures 2 and 3 respectively for uniform and nonlinear temperature rise (NTR) distributions. Similarly to the facts mentioned in previous studies, the neutral axis is first lifted away from the central axis as volume fraction index p increases from 0 to a value where the neutral axis reaches a maximum position. Then, after the highest position, the neutral axis starts to lower with a further increase in the p index. The highest position of the neutral axis depends on the elastic modulus ratio of constituent materials and temperature distribution, and it is about the value $p = 2$. The neutral axis position increases with temperature in uniform distribution and it is slowly decreasing with temperature rise in nonlinear distribution. Obviously, the neutral axis position under uniform temperature distribution is much greater than that under nonlinear distribution.

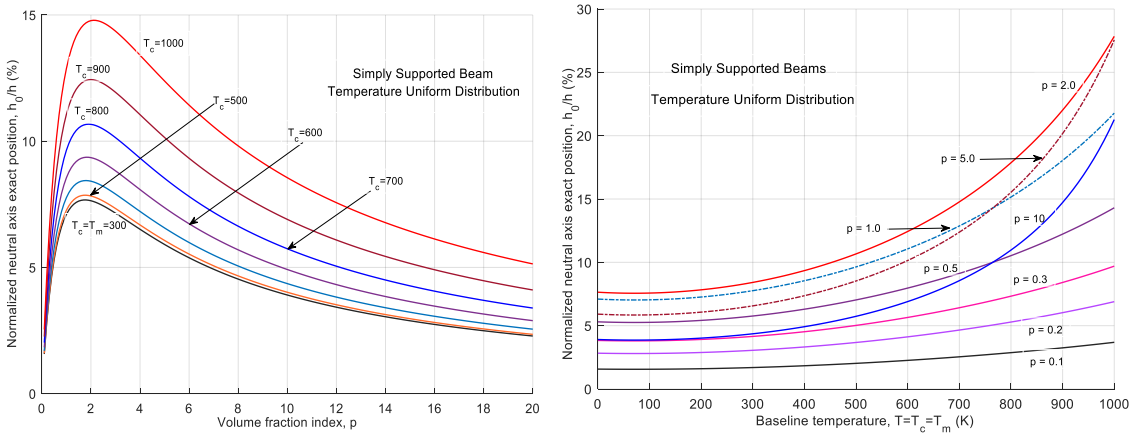

(a) (b)

Figure 2. Variation of neutral axis versus volume fraction index p (a) and temperature (b) for uniform temperature rise distribution.

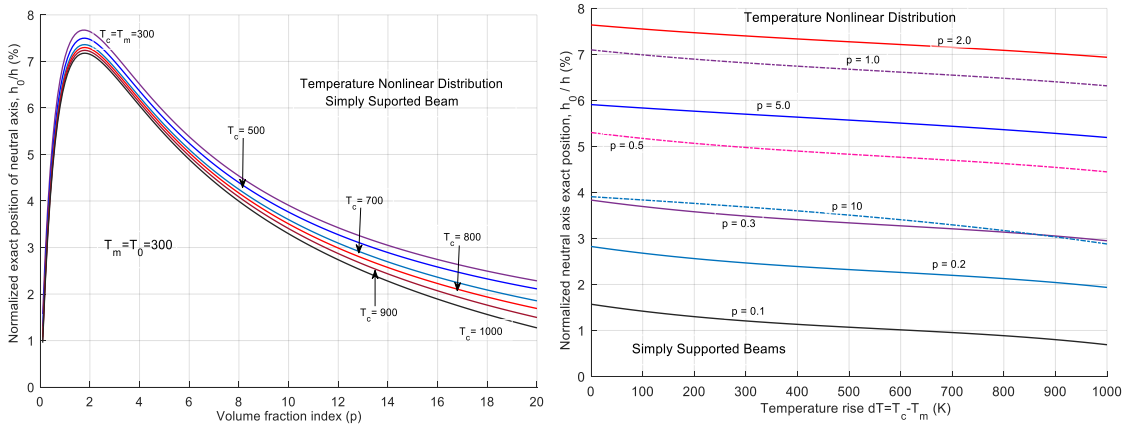

Figure 3. Variation of neutral axis versus volume fraction index p (a) and temperature rise (b) in nonlinear temperature distribution.

The NA-position computed by the linear temperature rise (LTR) distribution is shown in Figure 4(a) and difference between the neutral axis positions computed by LTR and NTR distributions are presented in Figure 4(b). Graphs in Figure 4(b) exhibit that the nonlinear temperature distribution gives neutral axis position computed higher than the linear distribution for a volume fraction index of more than 1 and difference between the LTR and NTR positions increases with temperature rise ΔT .

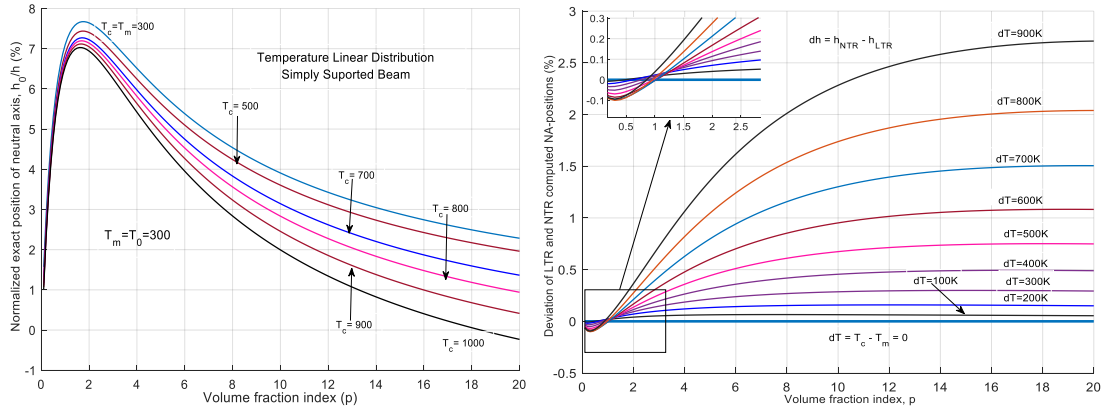

Figure 4. Variation of neutral axis versus volume fraction index p in linear temperature distribution (a) and its comparison to nonlinear distribution (b).

6.3. Variation of fundamental frequency

Fundamental frequency of SS-beam computed along volume fraction index and temperature rise using the neutral axis concept ($\bar{\omega}_{NA}$) and its deviation from that computed by central axis ($\bar{\omega}_{CA}$) are shown in Figures 5–6 for uniform and Figures 7–8 for nonlinear distributions. First, it is generally observed that the fundamental frequency of ceramic/metal FGM beams decreases with increasing volume fraction index, structure internal temperature, and thermal load of external environment. However, the frequency decreasing rate is significant

for small values (less than 2) of the material grading index regardless of whatever temperature or in case of high temperature and large volume fraction index (see Figures 5 and 7).

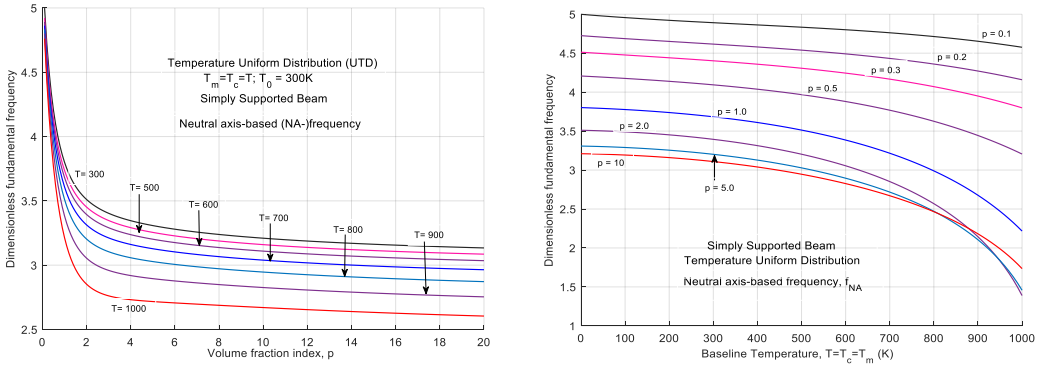

(a) (b)

Figure 5. Fundamental frequency computed along volume fraction index (a) and temperature rise (b) in uniform distribution using neutral axis for SS beam.

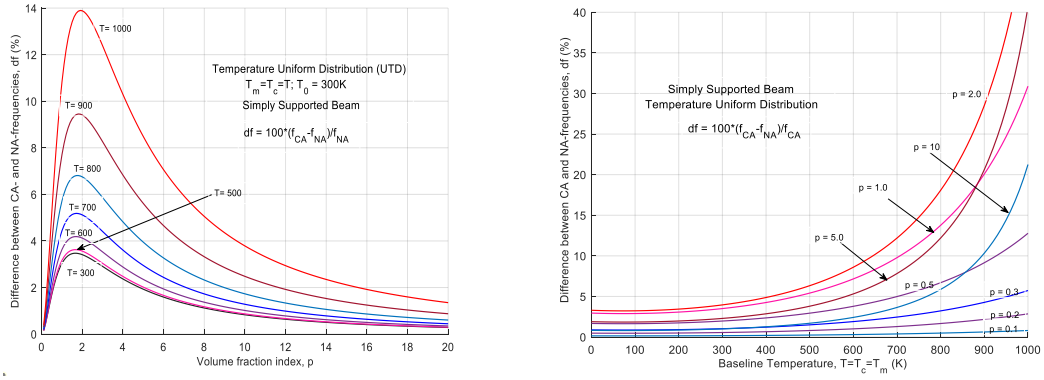

(a) (b)

Figure 6. Difference between NA- and CA-frequencies computed along volume fraction index (a) and baseline temperature (b) in uniform distribution for SS-Beams.

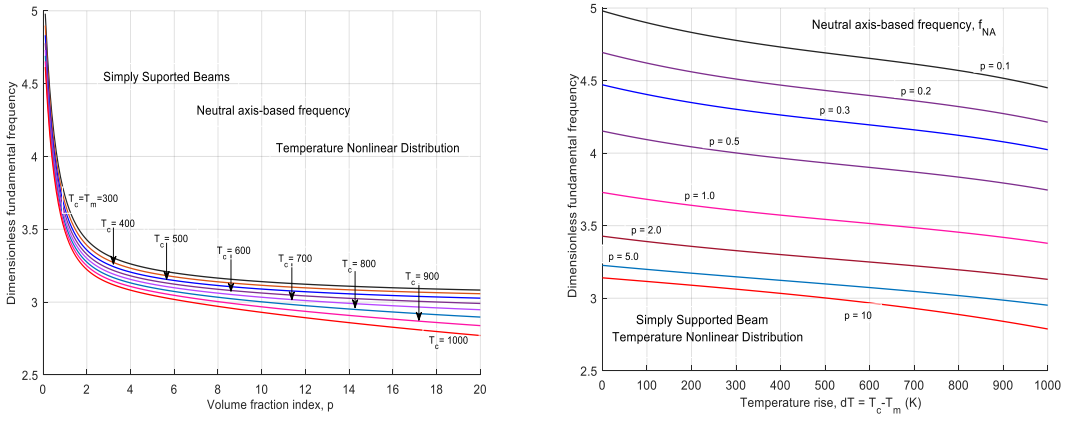

(a) (b)

Figure 7. Fundamental frequency computed along volume fraction index (a) and temperature rise (b) in nonlinear distribution using neutral axis for simply supported beam.

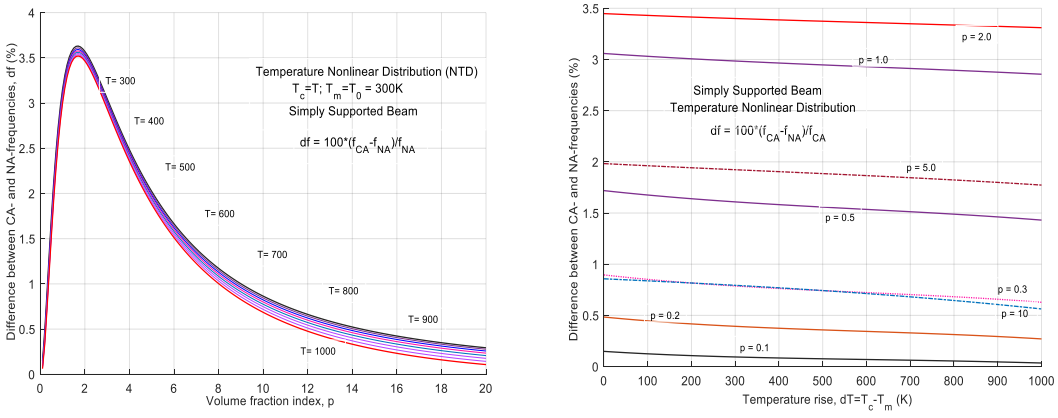

(a) (b)

Figure 8. Difference between NA- and CA-frequencies computed along volume fraction index (a) and temperature rise (b) in nonlinear distribution for SS-Beams.

Graphs in Figures 6 and 8 show that CA-frequency is consistently greater than NA-frequency and their deviation reaches a maximum at volume fraction index approximately close to 2. The change in fundamental frequency due to neutral axis used instead of central one increases rapidly with reference temperature in uniform distribution (Figure 6) and decreases slowly with temperature rise in nonlinear distribution (Figure 8). Finally, it can be noted that miscalculation of fundamental frequency using the central axis-based model of FGM beams may exceed 10 % for high temperature of uniform distribution, while it is not exceeded by 5 % in case of nonlinear temperature rise.

7. CONCLUSIONS

In this paper, the exact position of the neutral axis in a functionally graded beam with temperature-dependent properties has been obtained in an explicit expression of material constants including the thermo-elastic ones and used for examining its effect on the beam's fundamental frequency. Governing equations have been established using the classical beam theory, power law of material gradation, and steady-state heat conduction. Numerical analysis accomplished in this study allows one to draw the following conclusions:

As earlier well-known, both material gradation (volume fraction) index and temperature rise lead to a decrease of ceramic/metal beam's natural frequencies.

Dislocation of the neutral axis from the central one is strongly dependent upon the material gradation index and the temperature difference between top and bottom surfaces. Namely, the reference temperature of unform distribution field increases significantly the neural axis deviation from the central one.

Miscalculation of fundamental frequency of functionally graded beams based on central axis may exceed 10 % in case of uniform temperature distribution and reaches 5 % for nonlinear temperature rise distribution.

The exact position of the neutral axis must be accounted for vibration analysis of FGM beams, especially in the case of high temperature change and the volume fraction index ranged between 1 and 2.

The theoretical development proposed in this study can be used for numerical analysis of FGM beams with other ceramic on the top and other metal at the bottom with other boundary conditions.

Acknowledgements. This work has been completed in the framework of a cooperative project supported by Vietnam Academy of Science and Technology with Grant Number QTBY01.10/23-24 and Belarusian Republican Foundation for Fundamental Research under Granting Number F23V-013 dated 01.02.2023.

CrediT authorship contribution statement. Nguyen Ngoc Huyen: Investigation, Data curation, Validation. Do Nam: Software, Resources, Data curation. Vadim Kudryashov: Formal analysis, Supervision, Funding acquisition. Nguyen Tien Khiem: Conceptualization, Methodology, Investigation, Writing – original draft.

Declaration of competing interest: The authors declare that they have no known competing financial interests or personal relationships that could have appeared to influence the work reported in this paper.

REFERENCES

1. Birman V., Byrd L. M. - Modeling and Analysis of Functional Graded Materials and Structures. Appl. Mech. Rev., **60**(5) (2007) 195-216. https://doi.org/10.1115/1.2777164.
2. Zhong Z., Yu T. - Analytical solution of a cantilever functionally graded beam. Compos. Sci. Technol., **67**(3-4) (2007) 481-488. https://doi.org/10.1016/j.compscitech.2006.08.023.
3. Li X. F. - A unified approach for analyzing static and dynamic behaviors of functionally graded Timoshenko and Euler-Bernoulli beams. J. Sound Vib., **318**(4-5) (2008) 1210-1229. https://doi.org/10.1016/j.jsv.2008.04.056.
4. Sina S. A., Navazi H. M., Haddadpour H. - An analytical method for free vibration analysis of functionally graded beams. Mater. Des., **30**(3) (2009) 741-747. https://doi.org/10.1016/j.matdes.2008.05.015.
5. Şimşek M. - Fundamental frequency analysis of functionally graded beams by using different higher-order beam theory. Nucl. Eng. Des., **240**(4) (2010) 697-705. https://doi.org/10.1016/j.nucengdes.2009.12.013.
6. Alshorbagy A. E., Eltaher M. A., Mahmoud F. F. - Free vibration characteristics of a functionally graded beam by finite element method. Appl. Math. Model., **35**(1) (2011) 412-425. https://doi.org/10.1016/j.apm.2010.07.006.
7. Pradhan K. K., Chakraverty S. - Free vibration of Euler and Timoshenko functionally graded beams by Rayleigh-Ritz method. Compos. B: Eng., **51** (2013) 175-184. https://doi.org/10.1016/j.compositesb.2013.02.027.
8. Pradhan N., Sarangi S. K. - IOP Conference Series: Materials Science and Engineering, (2018) 012211. https://doi.org/10.1088/1757-899X/377/1/012211.
9. Chakraborty A., Gopalakrishnan S. - A spectrally formulated finite element for wave propagation analysis in functionally graded beams. Int. J. Solids Struct., **40**(10) (2003) 2421-2448. https://doi.org/10.1016/S0020-7683(03)00029-5.
10. Su H., Banerjee J. R. - Development of dynamic stiffness method for free vibration of functionally graded Timoshenko beams. Comput. Struct., **147** (2015) 107-116. https://doi.org/10.1016/j.compstruc.2014.10.001.
11. Yaghoobi H., Fereidoon A. - Influence of neutral surface position on deflection of functionally graded beam under uniform distributed load. World Appl. Sci. J., **10**(3) (2010) 337-341.
12. Eltaher M. A., Alshorbagy A. E., Mahmoud F. F. - Determination of neutral axis position and its effect on natural frequencies of functionally graded macro/nanobeams. Compos. Struct., **99** (2013) 193-201. https://doi.org/10.1016/j.compstruct.2012.11.039.

13. Chen W. R., Chang H. - Closed-form solution for free vibration frequencies of functionally graded Euler-Bernoulli beams. Mech. Compos. Mater., **53**(1) (2017) 79-98. https://doi.org/10.1007/s11029-017-9642-3.
14. Huyen N. N., Khiem N. T. - Modal analysis of functionally graded Timoshenko beam. Vietnam J. Mech., **39**(1) (2017) 31-50. https://doi.org/10.15625/0866-7136/7582.
15. Khiem N. T. - Vibration of Cracked Functionally Graded Beams: General Solution and Application – A Review. Vietnam J. Mech., **44**(4) (2022) 317-347. https://doi.org/10.15625/0866-7136/17986.
16. Touloukian Y. S. - Thermophysical properties of high temperature solid materials. Macmillan, New York (1967).
17. Reddy J. N., Chin C. D. - Thermomechanical Analysis of Functionally Graded Cylinders and Plates. J. Therm. Stresses, **21**(6) (1998) 593-626. https://doi.org/10.1080/01495739808956165.
18. Sankar B. V., Tzeng J. T. - Thermal stress in functionally graded beams. AIAA J., **40**(6) (2002) 1228-1232. https://doi.org/10.2514/2.1775.
19. Librescu L., Oh S. Y., Song O. - Thin-wall beams made of functionally graded materials and operating in a high temperature environment: Vibration and Stability. J. Therm. Stresses, **28**(6-7) (2005) 649-712. https://doi.org/10.1080/01495730590934038.
20. Abbasi M., Sabbaghian M., Eslami M. R. - Exact closed-form solution of the dynamic coupled thermoelastic response of a functionally graded Timoshenko beam. J. Mech. Mater. Struct., **5**(1) (2010) 79-94. https://doi.org/10.2140/jomms.2010.5.79.
21. Alshorbagy A. E. - Temperature effect on the vibration characteristics of a functionally graded thick beam. Ain Shams Eng. J., **4**(3) (2013) 455-464. https://doi.org/10.1016/j.asej.2012.11.001.
22. Chen Y., Jin G., Zhang C., Ye T., Xue Y. - Thermal vibration of FGM beams with general boundary conditions using a higher-order shear deformation theory. Compos. B: Eng., **153** (2018) 376-386. https://doi.org/10.1016/j.compositesb.2018.08.111.
23. Mahi A., Adda Bedia E. A., Tounsi A., Mechab I. - An analytical method for temperature-dependent free vibration analysis of functionally graded beams with general boundary conditions. Compos. Struct., **92**(8) (2010) 1877-1887. https://doi.org/10.1016/j.compstruct.2010.01.010.
24. Ebrahimi F., Ghasemi F., Salari E. - Investigating thermal effects on vibration behavior of temperature-dependent compositionally graded Euler beams with porosities. Meccanica, **51**(1) (2016) 223-249. https://doi.org/10.1007/s11012-015-0208-y.
25. Malekzadeh P., Monajjemzadeh S. M. - Dynamic response of functionally graded beams in thermal environment under moving load. Mech. Adv. Mater. Struct., **23**(3) (2015) 248-258. https://doi.org/10.1080/15376494.2014.949930.
26. Malekzadeh P., Shojaee A. - Dynamic response of functionally graded beams under moving heat source. J. Vib. Control, **20**(6) (2012) 803-814. https://doi.org/10.1177/1077546312464990.
27. Kiani Y., Eslami M. R. - Thermomechanical buckling oftemperature-dependent FGM beams. Lat. Am. J. Solids Struct., **10**(2) (2013) 223-246. https://doi.org/10.1590/S1679-78252013000200001.
28. Anandrao K. S., Gupta R. K., Ramchandran P., Rao G. V. - Thermal Buckling and Free Vibration Analysis of Heated Functionally Graded Material Beams. Def. Sci. J., **63**(3) (2013) 315-322. https://doi.org/10.14429/dsj.63.2370.
29. Trinh L. C., Vo T. P., Thai H.-T., Nguyen T.-K. - An analytical method for the vibration and buckling of functionally graded beams under mechanical and thermal loads. Compos. B: Eng., **100** (2016) 152-163. https://doi.org/10.1016/j.compositesb.2016.06.067.
30. Wattanasakulpong N., Gangadhara Prusty B., Kelly D. W. - Thermal buckling and elastic vibration of third-order shear deformable functionally graded beams. Int. J. Mech. Sci., **53**(9) (2011) 734-743. https://doi.org/10.1016/j.ijmecsci.2011.06.005.
31. Mojahedin A., Jabbari M., Rabczuk T. - Thermoelastic analysis of functionally Graded Porous Beam. J. Therm. Stresses, **41**(8) (2018) 937-950. https://doi.org/10.1080/01495739.2018.1446374.
32. Ebrahimi F., Salari E., Hosseini S. A. H. - Thermomechanical Vibration Behavior of FG nanobeams Subjected to Linear and Nonlinear Temperature Distribution. J. Therm. Stresses, **38**(12) (2015) 1360-1386. https://doi.org/10.1080/01495739.2015.1073980.
33. Kiani Y., Taheri S., Eslami M. R. - Thermal Buckling of Piezoelectric Functionally Graded Material Beams. J. Therm. Stresses, **34**(8) (2011) 835-850. https://doi.org/10.1080/01495739.2011.586272.

34. Kim Y.-W. - Temperature dependent vibration analysis of functionally graded rectangular plates. J. Sound Vib., **284**(3-5) (2005) 531-549. https://doi.org/10.1016/j.jsv.2004.06.043.
35. Shahrjerdi A., Mustapha F., Bayat M., Majid D. L. A. - Free vibration analysis of solar functionally graded plates with temperature-dependent material properties using second order shear deformation theory. J. Mech. Sci. Technol., **25**(9) (2011) 2195-2209. https://doi.org/10.1007/s12206-011-0610-x.
36. Xing Y. F., Wang Z. K., Xu T. F. - Closed-form Analytical Solution for Free Vibration of Rectangular Functionally Graded Thin Plates in Thermal Environment. Int. J. Appl. Mech., **10**(3) (2018) 1850025. https://doi.org/10.1142/S1758825118500254.
37. Lee Y.-H., Bae S.-I., Kim J.-H. - Thermal buckling behavior of functionally graded plates based on neutral surface. Compos. Struct., **137** (2016) 208-214. https://doi.org/10.1016/j.compstruct.2015.11.023.
38. Lim T.-K., Kim J.-H. - Thermo-elastic effects on shear correction factors for functionally graded beam. Compos. B: Eng., **123** (2017) 262-270. https://doi.org/10.1016/j.compositesb.2017.05.031.

APPENDIX

I. Calculation of integrals

First, it can be verified that the following integrals are easily calculated

$$\int_{-h/2}^{h/2} V^m(z)\,dz = \int_{-h/2}^{h/2} (z/h+1/2)^m\,dz = h\int_0^1 y^m dy = \frac{h}{(m+1)} \tag{A.1}$$

$$\int_{-h/2}^{h/2} V^m(z)\,z dz = \int_{-h/2}^{h/2} (z/h+1/2)^m\,z dz = h^2\int_0^1 y^m (y-1/2) dy = \frac{h^2 m}{2(m+1)(m+2)} \tag{A.2}$$

$$\int_{-h/2}^{h/2} V^m(z)\,z^2 dz = \int_{-h/2}^{h/2} (z/h+1/2)^m\,z^2 dz = h^3\int_0^1 y^m (y-1/2)^2 dy = \frac{h^3(m^2+m+2)}{4(m+1)(m+2)(m+3)} \tag{A3}$$

Therefore, for elasticity modulus determined by expression (33) one can calculate the integrals

$$\int_{-h/2}^{h/2} E(z,T)\,dz = h\psi_0\left(p,\bar{E}_0^t,\bar{E}_0^b,...,\bar{E}_3^t,\bar{E}_3^b\right);\ \int_{-h/2}^{h/2} E(z,T)\,z dz = h^2\psi_1\left(p,\bar{E}_0^t,...,\bar{E}_3^t,\bar{E}_0^b,...,\bar{E}_3^b\right);$$

$$\int_{-h/2}^{h/2} E(z,T)\,z^2 dz = h^3\psi_2\left(p,\bar{E}_0^t,...,\bar{E}_3^t,\bar{E}_0^b,...,\bar{E}_3^b\right) \tag{A4}$$

where

$$\psi_0\left(p,\bar{E}_k^t,\bar{E}_k^b\right) = \left\{\sum_{k=0}^{3}\sum_{n_1,...,n_k=0}^{\infty}\delta_{n_1}...\delta_{n_k}\frac{(m_k+1)\bar{E}_k^t + p\bar{E}_k^b}{(m_k+1)(m_k+1+p)}\right\} \tag{A.5}$$

$$\psi_1 = \left\{\sum_{k=0}^{3}\sum_{n_1,...,n_k=0}^{\infty}\delta_{n_1}...\delta_{n_k}\frac{(m_k+1)(m_k+2)(m_k+p)\bar{E}_k^t - p\left[2-m_k(m_k+p)\right]\bar{E}_k^b}{2(m_k+1)(m_k+2)(m_k+1+p)(m_k+2+p)}\right\}; \tag{A.6}$$

$$\psi_2 = \frac{1}{4}\sum_{k=0}^{3}\sum_{n_1,\ldots,n_k}^{\infty}\delta_{n_1}\ldots\delta_{n_k}\left[\frac{\left(m_k^2+m_k+2\right)\bar{E}_k^b}{\left(m_k+1\right)\left(m_k+2\right)\left(m_k+3\right)}+\frac{\left[\left(m_k+p\right)^2+\left(m_k+p\right)+2\right]\bar{E}_k^{t-b}}{\left(m_k+1+p\right)\left(m_k+2+p\right)\left(m_k+3+p\right)}\right]. \quad (A.7)$$

II. Calculation of mechanical constants

Using Eq. (A.4) the formulae (9) yields

$$A_{11} = b\int_{-h/2}^{h/2} E\left(z,T\right)dz = bh\psi_0\left(p,\bar{E}_0^t,\bar{E}_0^b,\ldots,\bar{E}_3^t,\bar{E}_3^b\right) \quad (A.8)$$

and

$$A_{22} = b\int_{-h/2}^{h/2} E(z,T)(z-h_0)^2dz = b\left[\int_{-h/2}^{h/2} E(z,T)\left(z^2-2zh_0+h_0^2\right)dz\right]$$

$$= b\left[\int_{-h/2}^{h/2} E(z,T)z^2dz - 2h^2h_0\psi_1 + hh_0^2\psi_0\right] = b\int_{-h/2}^{h/2} E(z,T)z^2dz - 2bh^2h_0\psi_1 + bhh_0^2\psi_0$$

Therefore, using the last equation in (34) we obtain

$$A_{22} = bh^3\left[\psi_2 - 2\bar{h}_0\psi_1 + \bar{h}_0^2\psi_0\right], \bar{h}_0 = h_0/h \quad (A.9)$$

Now, let's consider the case, when $\alpha_b(T) = \alpha_0^b\left(1+\alpha_1^bT\right), \alpha_t(T) = \alpha_0^t\left(1+\alpha_1^tT\right)$ that allows the expression $\alpha(z,T) = \alpha_b(T) + [\alpha_t(T) - \alpha_b(T)]V^p\left(z\right)$ to be written in the form

$$\alpha(z,T) = A_0^b + A_0^{t-b}V^p + \left(A_1^b + A_1^{t-b}V^p\right)\nabla T \quad (A.10)$$

where

$$A_0^b = \alpha_0^b\left(1+\alpha_1^bT_b\right); A_1^b = \alpha_0^b\alpha_1^bT_{t-b}; A_0^t = \alpha_0^t\left(1+\alpha_1^tT_b\right); A_1^t = \alpha_0^t\alpha_1^tT_{t-b}$$

$$A_0^{t-b} = \alpha_0^{t-b}\left(1+\alpha_1^{t-b}T_b\right) = A_0^t - A_0^b; A_1^{t-b} = \alpha_0^{t-b}\alpha_1^{t-b}T_{t-b} = A_1^t - A_1^b.$$

Next, substituting series (19) into (44) yields

$$\alpha(z,T) = A_0^b + A_0^{t-b}V^p + \sum_{n=0}^{\infty}\delta_n\left(A_1^bV^{np+1} + A_1^{t-b}V^{np+1+p}\right). \quad (A.11)$$

and in consequence one to obtains

$$E(z,T)\alpha(z,T)\Delta T == \sum_{k=1}^{5}\sum_{n_1,\ldots,n_k=0}^{\infty}\delta_{n_1}\ldots\delta_{n_k}\left\{R_{k-1}^{bb}V^{m_k} + R_{k-1}^{b(t-b)}V^{m_k+p} + R_{k-1}^{2(t-b)}V^{m_k+2p}\right\} \quad (A.12)$$

where the following notations have been introduced

$$R_0^{bb} = A_0^b\bar{E}_0^b; R_0^{b(t-b)} = A_0^{t-b}\bar{E}_0^b + A_0^b\bar{E}_0^{t-b}; R_0^{2(t-b)} = A_0^{t-b}\bar{E}_0^{t-b}$$

$$R_1^{bb} = A_0^b\bar{E}_1^b + A_1^b\bar{E}_0^b; R_1^{b(t-b)} = A_0^{t-b}\bar{E}_1^b + A_0^b\bar{E}_1^{t-b} + A_1^{t-b}\bar{E}_0^b + A_1^b\bar{E}_0^{t-b}; R_1^{2(t-b)} = A_0^{t-b}\bar{E}_1^{t-b} + A_1^{t-b}\bar{E}_0^{t-b}$$

$$R_2^{bb} = A_0^b\bar{E}_2^b + A_1^b\bar{E}_1^b; R_2^{b(t-b)} = A_1^{t-b}\bar{E}_1^b + A_1^b\bar{E}_1^{t-b} + A_0^{t-b}\bar{E}_2^b + A_0^b\bar{E}_2^{t-b}; R_2^{2(t-b)} = A_1^{t-b}\bar{E}_1^{t-b} + A_0^{t-b}\bar{E}_2^{t-b}$$

$$R_3^{bb} = A_0^b\bar{E}_3^b + A_1^b\bar{E}_2^b; R_3^{b(t-b)} = A_1^{t-b}\bar{E}_2^b + A_1^b\bar{E}_2^{t-b} + A_0^{t-b}\bar{E}_3^b + A_0^b\bar{E}_3^{t-b}; R_3^{2(t-b)} = A_1^{t-b}\bar{E}_2^{t-b} + A_0^{t-b}\bar{E}_3^{t-b}$$

$$R_4^{bb} = A_1^b \bar{E}_3^b; R_4^{b(t-b)} = A_1^{t-b} \bar{E}_3^b + A_1^b \bar{E}_3^{t-b}; \; R_4^{2(t-b)} = A_1^{t-b} \bar{E}_3^{t-b} \tag{A.13}$$
$$m_1 = np+1, m_2 = \left(n_1+n_2\right)p+2, \; m_3 = \left(n_1+n_2+n_3\right)p+3,$$
$$m_4 = \left(n_1+n_2+n_3+n_4\right)p+4, \; m_5 = \left(n_1+n_2+n_3+n_4+n_5\right)p+5$$

Therefore, it can be easy to calculate the integral

$$A_T = \int_{-h/2}^{h/2} E(z,T)\alpha(z,T)\nabla T dz = \sum_{k=1}^{5} \sum_{n_1,\ldots,n_k=0}^{\infty} \left[\frac{R_{k-1}^{bb}}{m_k+1} + \frac{R_{k-1}^{b(t-b)}}{m_k+p+1} + \frac{R_{k-1}^{2(t-b)}}{m_k+2p+1} \right] \tag{A.14}$$

Moreover, using similar formulas derived above for elastic constants A_{11}, A_{12}, A_{22}, we can calculate the independent upon temperature constants I_{11}, I_{12}, I_{22} as follows:

$$I_{11} = bh\frac{\rho_t + p\rho_b}{p+1}; I_{12} = \frac{bh^2}{p+1}\left[\frac{p\left(\rho_t - \rho_b\right)}{2\left(p+2\right)} - \bar{h}_0\left(\rho_t + p\rho_b\right) \right]$$

$$I_{22} = \frac{bh^3}{12\left(p+1\right)}\left[\frac{p\left(p^2+3p+8\right)\rho_b}{\left(p+2\right)\left(p+3\right)} - \frac{12p\left(\rho_t - \rho_b\right)\bar{h}_0}{\left(p+2\right)} + 12\left(\rho_t + p\rho_b\right)\bar{h}_0^2 \right] \tag{A.15}$$